# Gravitational waves from cosmological phase transitions

## Ruth Durrer

Département de Physique Théorique, Université de Genève 24 Quai E. Ansermet, 1211 Genéve 4, Switzerland

E-mail: ruth.durrer@unige.ch

**Abstract.** In this talk I discuss the generation of a stochastic background of gravitational waves during a first order phase transition. I present simple general arguments which explain the main features of the gravitational wave spectrum like the  $k^3$  power law growth on large scales and a estimate for the peak amplitude. In the second part I concentrate on the electroweak phase transition and argue that the nucleosynthesis bound on its gravitational wave background seriously limits seed magnetic fields which may have been generated during this transition.

#### 1. Introduction

The Universe has expanded and cooled down from a very hot initial state to (presently) 2.7°K. It seems likely that it underwent several phase transitions during its evolution of adiabatic expansion. It has already been proposed in the 80ties, that a cosmological phase transition can lead to the generation of a stochastic gravitational wave background [1]. If the phase transitions are of second order or only a crossover as it has been obtained from standard model calculations, we do not expect them to lead to an observable cosmological signal. However, if a phase transition is first order, it proceeds via bubble nucleation which is a highly inhomogeneous process. Some of the kinetic energy of the rapidly expanding bubbles is transferred to the cosmic plasma and leads to turbulence. If small seed magnetic fields are present, they are amplified by the turbulent motion which becomes MHD turbulence. Since the fluid and magnetic Reynolds numbers in the hot cosmic plasma are extremely high, MHD turbulence persists even after the phase transition, where it freely decays. These inhomogeneities int the energy and momentum of the cosmic plasma generate a stochastic background of gravitational waves. Here we want to investigate this background.

# 1.1. Events in the early Universe

The following important events have most probably taken place in the early Universe and they may, under certain circumstances have induced a background of stochastic gravitational waves.

• Inflation is supposed to have generated the scalar fluctuations in the geometry and energy density which have led to the observed anisotropies in the cosmic microwave background (CMB) [2, 3]. Simple inflationary models do not only induce scalar perturbations but the quantum fluctuations in the gravitational spin-2 degrees of freedom also lead to a scale invariant background of gravitational waves of similar amplitude. It is one of the most

important goals of present CMB experiments like Planck [4] to observe the B-polarization which this gravitational wave background should induce in the CMB photons.

Pre-heating: At the end of inflation the inflation decays into other degrees of freedom which eventually reheat the Universe and lead to a thermal bath of relativistic degrees of freedom containing especially also the standard model particles. The details of this process are complicated and in some cases they generate inhomogeneities leading to a significant stochastic background of gravitational waves [5]. Using the standard relation between temperature and time in a Friedmann Universe filled with relativistic particles [3], we obtain for a reheat temperature  $T_i$ 

$$T_i \simeq 10^{14} \text{GeV}, \quad t_i = 2.3 \text{sec} \left(\frac{1 \text{MeV}}{T_i}\right)^2 g_{\text{eff}}(T)^{-1/2} \simeq 10^{-32} \text{sec},$$
 (1)

$$\eta_i = \frac{1}{a(t_i)H(t_i)} = 2t_i(1+z_i) \simeq 10^{-7} \text{sec}, \quad \omega_i \gtrsim \frac{1}{\eta_i} \simeq 10^7 \text{Hz},$$
(2)

 $g_{\text{eff}}(T)$  denotes the effective number of relativistic degrees of freedom at temperature T [3]. To find the conformal time  $\eta_i$  we have used that in a radiation dominated universe

$$\eta = \frac{1}{\mathcal{H}} = \frac{1}{aH} = \frac{1+z}{H} = 2t(1+z),$$

where  $\mathcal{H} = aH$  is the comoving Hubble rate and a is the scale factor normalized to one today,  $a(t_0) = 1$ . Furthermore, since  $g_{\text{eff}}(aT)^3$  is constant during adiabatic expansion

$$1 + z = \frac{1}{a} = \frac{g_{\text{eff}}^{1/3} T}{g_0^{1/3} T_0} = \frac{10^{10}}{2.35} \left(\frac{T}{1 \text{MeV}}\right) \left(\frac{g_{\text{eff}}}{2}\right)^{1/3} \,,$$

so that

$$\eta = 0.67 \times 10^{10} \left(\frac{T}{1 \text{MeV}}\right) g_{\text{eff}}^{1/3} t \simeq 1.5 \times 10^{10} \text{sec} \left(\frac{1 \text{MeV}}{T}\right) g_{\text{eff}}(T)^{-1/6} .$$
(3)

We have set  $k_B = 1$  and measure temperature in MeV. In the following we use units with  $c = \hbar = 1$  so that length and time have the same units as inverse energy.

For the  $\gtrsim$  sign in eq. (2) we have used that the typical frequency generated by such an event must be larger than the inverse of the correlation scale which is always smaller than the horizon size at the given epoch. Note that  $\omega_i$  denotes the comoving frequency and we have normalized the scale factor to unity today, so that co-moving frequencies, length scales and times correspond to physical scales today.

So far no experiment which can detect gravitational waves with frequencies as high as  $\omega_i$ has been proposed.

The electroweak transition: In the standard model, for realistic values of the Higgs mass, the electroweak transition is not even second order, but only a crossover [6]. However, small deviations from the standard model e.g. in the Higgs sector or supersymmetric models [7] can can lead to a first order electroweak phase transition at temperature

$$T_{ew} \simeq 10^2 \text{GeV}, \qquad t_{ew} \simeq 10^{-10} \text{sec},$$
 (4)  
 $\eta_{ew} \simeq 10^5 \text{sec}, \qquad \omega_{ew} \gtrsim 10^{-5} \text{Hz}.$  (5)

$$\eta_{ew} \simeq 10^5 \text{sec}, \qquad \omega_{ew} \gtrsim 10^{-5} \text{Hz}.$$
(5)

If the electroweak phase transition is strongly first order, the bubbles expand very rapidly and the duration of the phase transition is a small fraction, maybe 1% of the Hubble time. In this case one expects a peak frequency of  $\omega_{ew} \sim 100/\eta_{ew} \simeq 10^{-3} \text{Hz}$ . This is the frequency of best sensitivity for the gravitational wave satellite LISA proposed for launch in 2018 [8]. • Confinement transition: Also in this case, standard lattice QCD calculations [9] predict a simple crossover. However, the confinement transition can be first order if the neutrino chemical potentials are sufficiently large (still within the limits allowed by nucleosynthesis) [10]. Models which lead to such high neutrino chemical potentials have been proposed for leptogenesis with sterile neutrini [11]. The temperature of the QCD transition is about

$$T_c \simeq 10^2 \text{MeV}, \quad t_c \simeq 10^{-5} \text{sec},$$
 (6)

$$\eta_c \simeq 10^7 \text{sec}, \quad \omega_c \gtrsim 10^{-7} \text{Hz}.$$
(7)

Gravitational waves in this frequency range could be observed by the pulsar timing array which has been proposed recently [12].

• Surprises: Last but not least we may hope to find a gravitational wave background from a phase transition at some other not predicted temperature which then would indicate new physics at the corresponding energy scale, see, e.g [13]. For example, a first order phase transition at a critical temperature  $T_* \simeq 10^7 \text{GeV}$  may lead to a gravitational wave background with a peak frequency of about 100Hz which is the best sensitivity of LIGO. As we shall argue below, in a very optimistic scenario it is even conceivable that such a background might be detected by the advanced configuration of the LIGO [14] experiment.

A more comprehensive overview on first order phase transitions as sources for gravitational waves can be found in Ref. [15].

In the following we present a semi-analytical determination of the gravitational wave (GW) signal from a first order phase transition in terms of a few free parameters. We then apply our general results to the electroweak phase transition and discuss some consequences.

#### 2. General results

Before we outline their derivation, let us present the main results. We consider a phase transition at  $T = T_*$  which generates (relativistic) anisotropic stresses which source gravitational waves. We assume that the energy density of this source is  $\rho_X$ . Since the source is relativistic its anisotropic stresses are of the same order of magnitude. The GW spectrum then has the following main properties:

- The peak frequency (the inverse of the correlation scale) is larger than the Hubble rate,  $k_* \gtrsim \mathcal{H}_*$ . Here we always compare comoving quantities which become physical scales today.
- The GW energy density is of the order of

$$\Omega_{gw}(\eta_0) \sim \epsilon \Omega_{\text{rad}}(\eta_0) \left(\frac{\Omega_X(\eta_*)}{\Omega_{\text{rad}}(\eta_*)}\right)^2 \quad \text{where}$$

$$\epsilon = \begin{cases} (\mathcal{H}_* \Delta \eta_*)^2 & \text{if } \mathcal{H}_* \Delta \eta_* < 1\\ 1 & \text{if } \mathcal{H}_* \Delta \eta_* \ge 1. \end{cases}$$
(8)

Here  $\Delta \eta_*$  is the duration over which the source is active, typically the duration of the phase transition.  $\Omega$  is the density parameter,  $\Omega_X = \rho_X/\rho_c$  where  $\rho_X$  is the energy density of the component X and  $\rho_c$  is the critical density.

• On large scales,  $k \ll k_*$  the spectrum is blue,

$$\frac{d\Omega_{gw}(k)}{d\log(k)} \propto k^3$$
,  $\Omega_{gw} = \int \frac{dk}{k} \frac{d\Omega_{gw}(k)}{d\log(k)}$ .

The second equality defines the gravitational wave energy per logarithmic frequency interval,  $\frac{d\Omega_{gw}(k)}{d\log(k)}$ .

• On small scales,  $k \gg k_*$  the spectrum decays. The decay law depends on the details of the source. If the anisotropic stress spectrum of the source decays with power  $k^{-\gamma}$ , and the source is totally coherent in time (see below), the gravitational wave energy density decays like  $k^{-(\gamma+1)}$ . If the source is coherent for about one wavelength, the gravitational wave energy density decays like  $k^{-(\gamma-1)}$  and if the source is incoherent, the gravitational wave energy density decays like  $k^{-(\gamma-3)}$ . see Ref. [17]. The unequal time correlator of the source is discussed in the next section.

# 3. Generation of gravitational waves

Gravitational waves are sourced by fluctuations in the energy momentum tensor which have a non-vanishing spin-2 contribution. The perturbed metric is of the form

$$ds^{2} = a^{2} \left( -d\eta^{2} + (\gamma_{ij} + 2h_{ij}) dx^{i} dx^{j} \right) , \qquad (9)$$

where  $\gamma_{ij}$  is the metric of a 3-space of constant curvature K and  $h_{ij}$  is transverse and traceless. In Fourier space  $k^i h_{ij} = h_i^i = 0$ .

Einstein's equation to first order in  $h_{ij}$  gives (we set K=0 in what follows)

$$\left(\partial_{\eta}^{2} + 2\mathcal{H}\partial_{\eta} + k^{2}\right)h_{ij} = 8\pi G a^{2}\Pi_{ij}.$$
(10)

Here  $\Pi_{ij}(\mathbf{k},\eta)$  is the Fourier component of the tensor type (spin-2) anisotropic stress of the source and  $\mathcal{H} = \frac{a'}{a}$ . A prime denotes the derivative w.r.t. conformal time  $\eta$ .

During a first order phase transition, anisotropic stresses can be generated by colliding bubbles and by inhomogeneities in the cosmic fluid (e.g. turbulence, magnetic fields) [16].

For a duration of the phase transition given by  $\Delta \eta_*$ , the final bubble size, i.e. the typical size of the bubbles when they start to coalesce and the phase transition terminates, is  $R_* = v_b \Delta \eta_*$ , where  $v_b$  is the bubble velocity. Typically  $\Delta \eta_* < \mathcal{H}^{-1}$ . As we shall see, depending on the unequal time correlation properties of the anisotropic stress, the peak frequency can be given either by the time scale,  $k_* \simeq (\Delta \eta_*)^{-1}$ , or by the spatial scale  $k_* \simeq R_*^{-1}$ . For the most promising case of a strongly first order phase transition, the bubble velocity is however close to the speed of light,  $v_b \simeq 1$  so that this distinction is not very relevant.

# 4. The spectrum

Because of causality, the correlator  $\langle \Pi_{ij}(\eta_1, \mathbf{x})]\Pi_{lm}(\eta_2, \mathbf{y})\rangle = \mathcal{M}_{ijlm}(\eta_1, \eta_2, \mathbf{x} - \mathbf{y})$  is a function of compact support. For distances  $|\mathbf{x} - \mathbf{y}| > \max(\eta_1, \eta_2)$ ,  $\mathcal{M} \equiv 0$ . Therefore, the spatial Fourier transform,  $\mathcal{M}_{ijlm}(\eta_1, \eta_2, \mathbf{k})$  is analytic in  $\mathbf{k}$  around  $\mathbf{k} = 0$ . We decompose  $\Pi_{ij}$  into two helicity modes which we assume to be uncorrelated so that the spectrum is even under parity

$$\Pi_{ij}(\eta, \mathbf{k}) = e_{ij}^{+} \Pi_{+}(\eta, \mathbf{k}) + e_{ij}^{-} \Pi_{-}(\eta, \mathbf{k})$$

$$\langle \Pi_{+}(\eta, \mathbf{k}) \Pi_{+}^{*}(\eta', \mathbf{k}') \rangle = \langle \Pi_{-}(\eta, \mathbf{k}) \Pi_{-}^{*}(\eta', \mathbf{k}') \rangle = (2\pi)^{3} \delta^{3}(\mathbf{k} - \mathbf{k}') \rho_{X}^{2} P_{\Pi}(\eta, \eta', \mathbf{k})$$

$$\langle \Pi_{+}(\eta, \mathbf{k}) \Pi_{-}^{*}(\eta', \mathbf{k}') \rangle = 0.$$

Here  $\rho_X$  is the energy density of the component X with anisotropic stress  $\Pi$  which has been factorized in order to keep  $k^3 P_{\Pi}(\eta, \eta', k)$  dimensionless. Causality implies that the function  $P_{\Pi}(\eta, \eta', k)$  is analytic in k. We therefore expect it to start out as white noise and to decay beyond a certain correlation scale  $k_*(\eta, \eta') > \min(1/\eta, 1/\eta')$ .

If the gravitational wave source is active only for a short duration  $\Delta \eta_*$  (less than one Hubble time), we can neglect the damping term  $2\mathcal{H}$  in the equation of motion for h during the time when  $\Pi$  is active. Here h denotes either of the two helicities of the gravitational wave and  $\Pi$  is

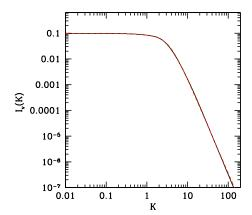


Figure 1. The equal time anisotropic stress power spectrum from turbulence. On large scales the spectrum is scale invariant, on scales much smaller than the correlation scale it falls of like  $k^{-11/3}$  which is determined by the Kolmogorov turbulence assumed for the velocity power spectrum. The black line is the numerical result and the red dashed line a simple fit. The normalization is arbitrary. Figure from [17].

the anisotropic stress source of the corresponding helicities. The solution with vanishing initial conditions is then

$$h(\mathbf{k}, \eta) = \frac{8i\pi G a_*^3}{6ak} \left[ e^{-ik\eta} \int_{\eta_*}^{\eta_* + \Delta \eta_*} d\eta' e^{ik\eta'} \Pi(\eta', \mathbf{k}) + e^{ik\eta} \int_{\eta_*}^{\eta_* + \Delta \eta_*} d\eta' e^{-ik\eta'} \Pi(\eta', \mathbf{k}) \right]$$
$$= \frac{8i\pi G a_*^3}{6ak} \left[ e^{-ik\eta} \Pi(k, \mathbf{k}) + e^{ik\eta} \Pi(-k, \mathbf{k}) \right], \qquad \eta > \eta_* + \Delta \eta_*.$$

The gravitational wave energy density is given by

$$\rho_{gw}(\eta, \mathbf{x}) = \frac{1}{32\pi G a^2} \langle \partial_{\eta} h_{ij}(\eta, \mathbf{x}) \partial_{\eta} h_{ij}^*(\eta, \mathbf{x}) \rangle.$$

If the Universe is radiation dominated at the time  $\eta_*$  when the gravitational waves are generated, this leads to the gravitational wave energy spectrum

$$\frac{d\Omega_{gw}}{d\ln(k)}(\eta_0) = \frac{12\Omega_{\rm rad}(\eta_0)}{\pi^2} \left(\frac{\Omega_X(\eta_*)}{\Omega_{\rm rad}(\eta_*)}\right)^2 \mathcal{H}_*^2 k^3 \operatorname{Re}[P_{\Pi}(k,k,k)]. \tag{11}$$

Here

$$P_{\Pi}(\omega,\omega',k) \equiv \int_{-\infty}^{-\infty} d\eta \int_{-\infty}^{-\infty} d\eta' P_{\Pi}(\eta,\eta',k) e^{i(\omega\eta-\omega'\eta')}. \tag{12}$$

On large scales,  $k < k_*$  the GW energy density from a 'causal' source always scales like  $k^3$ . This remains valid also for long duration sources. The only change for long lived sources is that the Green function  $e^{ik(\eta-\eta')}$  of the wave operator in Minkowski spacetime has to be replaced by the Green function of the wave operator in an expanding universe which in the case of a radiation dominated universe is given in terms of spherical Bessel functions.

The scale  $1/k_*$  is the correlation scale which is smaller than the co-moving Hubble scale  $1/k_* < 1/\mathcal{H}_* = \eta_*$ . The behavior or the spectrum close to the peak and its decay rate on

smaller scales depend on the source characteristics, on its temporal behavior and on its power spectrum.

Let us now briefly discuss the different results which have been obtained for the position of the peak of the gravitational wave spectrum. As we see from eqs. (12) and (11), to determine the the gravitational wave energy density we must know the unequal time correlator of the of the anisotropic stresses,  $P_{\Pi}(\eta, \eta', k)$ . This is not well known from numerical simulations but there exist different simple possibilities:

• A totally coherent source is one for which the time dependence is deterministic. In this case the randomness is solely in the initial conditions and  $\Pi(\eta, \mathbf{k}) = f(\eta, k)\Pi(\eta_*, \mathbf{k})$  for some deterministic function f. For the unequal time correlator  $P_{\Pi}$  this leads to

$$P_{\Pi}(\eta, \eta', k) = \sqrt{P_{\Pi}(\eta', \eta', k)P_{\Pi}(\eta, \eta, k)}.$$

It has been shown in Refs. [18, 17] that the peak position of the GW spectrum  $\propto k^3 P_{\Pi}(k,k,k)$  for a totally coherent source is given by the peak of the temporal Fourier transform of the source, i.e.  $k_* = (\Delta \eta_*)^{-1}$ .

• For a source with finite coherence time we can model the unequal time correlator of the of the anisotropic stresses, by

$$P_{\Pi}(\eta, \eta', k) = \sqrt{P_{\Pi}(\eta', \eta', k)P_{\Pi}(\eta, \eta, k)}\Theta(x_c - | \eta - \eta' | k), \quad x_c \sim 1.$$

This ansatz assumes that the source is totally coherent if the time difference is smaller than about one wavelength and uncorrelated for larger time differences. This ansatz resembles the suggestion by Kraichnan [19] for turbulence and has therefore been used for both turbulence and magnetic fields in Ref. [17]. However, this ansatz, like also the Kraichan decorrelation ansatz still lacks numerical confirmation.

In this case, the peak of the GW spectrum is determined by the peak of the *spatial* Fourier transform of the source.

• A totally incoherent source is uncorrelated for different times. Its unequal time correlator can be modeled as

$$P_{\Pi}(\eta, \eta', k) = P_{\Pi}(\eta', \eta', k) \Delta \eta_* \delta(\eta - \eta').$$

Here the factor  $\Delta \eta_*$  is present to make the dimensions right, it can be replaced by some other short correlation time. In this case, the GW spectrum is also determined by the peak of the *spatial* Fourier transform of the source.

The resulting gravitational wave spectra from the different hypotheses for the unequal time correlator are shown in Fig. 2. They are derived in detail in Ref. [17].

# 5. The electroweak phase transition

According to the standard model, the electroweak transition is not even second order, but only a cross-over. Then, this transition does not lead to the formation of gravitational waves. Even though the Higgs vacuum expectation value does cross-over from zero to a finite value, the corresponding Higgs field fluctuations have a very short correlation length of the order of the inverse temperature and do not invoke significant gravitational field fluctuations.

However, if the standard model is somewhat modified e.g. in the Higgs sector, or in certain regions of the MSSM parameter space, the electroweak phase transition can become first order, even strongly first order [7]. Then it proceeds via the formation of large bubbles of true vacuum. The bubbles themselves are spherically symmetric and do not generate gravitational waves but the collision events do.

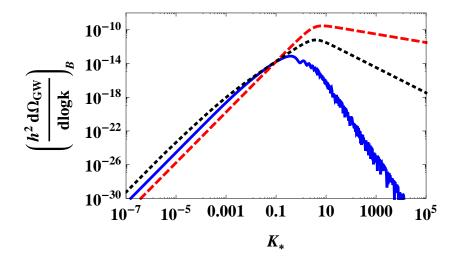


Figure 2. The GW energy density spectrum for a totally incoherent source (red, long-dashed), a totally coherent source (blue solid) and for a source with finite coherence time (black, short-dashed). The parameters are:  $T_* = 100 \text{ GeV}$ ,  $\Delta \eta_* \mathcal{H}_* = 0.01$ ,  $\Omega_X/\Omega_{\rm rad} = 2/9$  ( $\langle v^2 \rangle = 1/3$ ). The horizontal variable is  $K_* = kR_*/(2\pi)$ . Note that the peak position is roughly at  $k = \pi/\Delta \eta_* =$  a few, hence  $K_* \simeq R_*/\Delta \eta_* = v_b$  in the totally coherent case and at  $k = \pi/R_* = a$  few, hence  $K_* \simeq 1$  in the incoherent case and in the case with finite coherence length. In order to clearly separate the peak positions,  $v_b \simeq 0.1$  has been chosen. Figure from [17].

In addition, the Reynolds number of the cosmic plasma is very high and the bubbles are expected to induce turbulence and, if there are small magnetic seed fields these are amplified by turbulence leading to an MHD turbulent plasma with turbulent kinetic energy and magnetic fields in equipartition [20].

The correlation scale is expected to be [21] of the order of  $k_* = \beta = (\Delta \eta_*)^{-1} \simeq 100/\eta_* \sim 10^{-3}$ Hz, which is close to the frequency of the peak sensitivity for the space born gravitational wave antenna LISA, proposed for launch in 2018 by ESA [8].

#### 5.1. Bubble collisions

New numerical simulations of gravitational waves from bubble collisions during the electroweak phase transition [22] have given a slower decay law on small scales, like  $\propto k^{-1}$ , see Fig. 3.

In Ref. [18] it has been shown that the decays law  $\frac{d\Omega_{gw}(k)}{d\log k} \propto k^{-1}$  is generically expected on small scales (large k) if  $P_{\Pi}(\eta, \eta, k)$  is continuous in time but not differentiable. This behavior seems reasonable for bubble collisions which start from vanishing overlap continuously but with a finite slope.

## 5.2. Turbulent MHD

Since the Reynolds number Re, of the cosmic plasma at  $T \sim 100 \text{GeV}$  is very high, the rapidly expanding bubbles of the broken phase provoke the formation of turbulence. Furthermore, in the broken phase the electromagnetic field does generically not vanish. Since the magnetic Reynolds number  $R_m$  is even higher than the Reynolds number of the plasma [17], and thus the Prandl number [20]  $P_m = R_m/Re \gg 1$ , the high conductivity rapidly damps the electric fields and we are left with a magnetic field in a turbulent plasma, MHD turbulence [20].

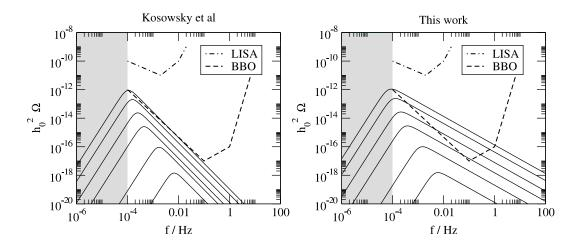


Figure 3.  $\frac{d\Omega_{gw}(f)}{d\log f}$  from colliding bubbles,  $f = k/2\pi$ , numerical results for  $\Omega_X/\Omega_{\rm rad} = 0.03$ . On the left panel the old results from Ref. [16] are shown while the right panel shows the result of Ref. [22]. Figure from [22].

To determine the anisotropic stress tensors from the turbulent flow and from the magnetic field which is the source of gravitational waves, we first discuss the vorticity and magnetic field spectra. Because both, the vorticity and the magnetic field are divergence free, causality requires that their spectra behave like  $k^2$  for small k:

$$\langle v_i(\mathbf{k})v_j(\mathbf{k}')\rangle = (2\pi)^3 \delta^3(\mathbf{k} - \mathbf{k}')(\hat{k}_j \hat{k}_i - \delta_{ij}) P_v(k), \qquad (13)$$

$$\langle B_i(\mathbf{k})B_j(\mathbf{k}')\rangle = (2\pi)^3 \delta^3(\mathbf{k} - \mathbf{k}')(\hat{k}_j\hat{k}_i - \delta_{ij})P_B(k).$$
 (14)

The functions  $(\hat{k}_j\hat{k}_i - \delta_{ij})P_{\bullet}(k)$  must be analytic at k=0 because of causality (the correlation functions are functions with compact support, they vanish for separations larger than the Hubble scales, thus their Fourier transforms must be analytic) hence  $P_v(k)$  and  $P_B(k) \propto k^2$  for small k, see [23]. Turbulence is steered during the phase transition and then decays freely with decay time of the order of  $\Delta\eta_*$ . This source is not truly long-lived, but since it decays only like a power law and not exponentially, it does still contribute significantly for  $\eta > \eta_* + \Delta\eta_*$  and we expect a suppression factor  $\epsilon$  in eq. (8) which is larger than the naive factor  $(\mathcal{H}_*\Delta\eta_*)^2$ .

The behavior of the spectrum on scales smaller than the correlation scale  $k > k_*$  is expected to be a Kolmogorov spectrum for the vorticity field,  $P_v \propto k^{-11/3}$  and an Iroshnikov-Kraichnan spectrum [24] for the magnetic field,  $P_B \propto k^{-7/2}$ . For the induced GW spectrum this yields

$$\frac{d\Omega_{GW\bullet}(k,\eta_0)}{d\ln(k)} \simeq \epsilon \ \Omega_{\rm rad}(\eta_0) \left(\frac{\Omega_{\bullet}(\eta_*)}{\Omega_{\rm rad}(\eta_*)}\right)^2 \times \left\{ \begin{array}{ll} (k/k_*)^3 & \text{for } k \ll k_* \\ (k/k_*)^{-\alpha} & \text{for } k \gg k_* \,. \end{array} \right.$$

For  $\bullet = v$  we have  $\alpha = 11/3 - 1 = 8/3$  and for  $\bullet = B$  we have  $\alpha = 7/2 - 1 = 5/2$ , see [25]. To find  $\alpha$  we use that on small scale we expect the anisotropic stress spectrum to decay like the velocity, respectively magnetic field spectrum. With  $\langle |\dot{h}|^2 \rangle \propto P_{\Pi}/k^2$  and  $\frac{d\Omega_{gw}(k)}{d\ln(k)} \propto k^3 \langle |\dot{h}|^2 \rangle \propto k P_{\Pi}$  so that  $\alpha = \gamma - 1$ , where  $\gamma$  denotes the decay exponent of the anisotropic stress spectrum.

In Figs. 4 and 5 the gravitational spectrum obtained from the wheetroweak phase transityion and from a first order phase transition at  $T_* = 5 \times 10^6$  GeV are shown and compared with future gravitational wave experiments like LISA [8], the Bib Bang Observer (BBO) [26] asnd advances LIGO [14].

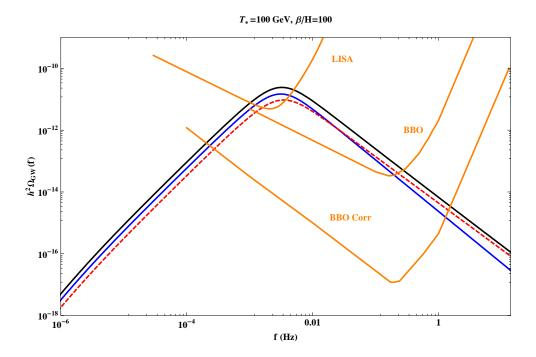


Figure 4. The gravitational wave energy density from magnetic fields (red) and turbulence (blue, the sum is shown in black) generated during the electroweak phase transition at  $T_* = 100 \text{GeV}$ . The time-decorrelation of the source is modeled by the finite correlation approach (Kraichnan decorrelation). The source energy density spectrum is assumed to be maximal,  $\Omega_v/\Omega_{\rm rad} = 2/9$ , see [17]. Equipartition in turbulent kinetic energy and magnetic field energy is assumed. The sensitivity curves are from [27]. Figure taken from [17].

# 5.3. Limits of primordial magnetic fields from the EW transition

It is difficult to estimate  $\Omega_B(\eta_*)$  or  $\Omega_v(\eta_*)$  directly, but since causality requires the spectra to be so blue, the limit on gravitational waves which comes from small scales  $k \simeq k_*$ , yields very strong limits on primordial magnetic fields on large scales already from the simple nucleosynthesis constraint,  $\Omega_{gw} \lesssim 0.1\Omega_{\rm rad}$ . If the magnetic field spectrum behaves like  $P_B(k) \propto k^n$ , the gravitational wave energy density per log interval must go like  $\frac{d\Omega_B(k,\eta_*)}{d\ln(k)} \propto k^{3+n}$  on large scales. For causal magnetic fields we have n=2, hence the magnetic field energy spectrum is very blue,

$$\frac{d\Omega_B(k, \eta_*)}{d\ln(k)} \propto k^5 \quad \text{for} \quad k < k_*. \tag{15}$$

The main contribution to the gravitational wave energy density comes from the correlation scale,  $\Omega_{gw} \simeq \frac{d\Omega_{gw}(k_*)}{d\ln(k_*)}$ , whereas we are interested in the magnetic fields on much larger scales, for example  $k_L = (0.1 \mathrm{Mpc})^{-1}$ . Using our simple formula (8) with  $\epsilon \sim 1$  the nucleosynthesis limit yields  $k_*^{3/2}B(k_*,\eta_0) \lesssim 10^{-6}\mathrm{Gauss}$ . The time  $\eta_0$  denotes today. For the electroweak phase transition  $k_* \simeq 100\mathcal{H}_* \simeq 10^{-3}\mathrm{sec}^{-1}$  while we are interested in magnetic fields on scales of 0.1Mpc giving  $k_L = 10(\mathrm{Mpc})^{-1} \simeq 10^{-13}\mathrm{sec}^{-1}$ . With the above scaling, the limit on a magnetic field on this scale is

$$k_L^{3/2}B(k_L, \eta_0) \lesssim \left(\frac{k_L}{k_*}\right)^{5/2} 10^{-6} \text{Gauss} = 10^{-31} \text{Gauss}.$$
 (16)

Note also that this limit is very stable with respect to the small unknown pre-factor  $\epsilon$ . Since  $\Omega_{qw} \propto B^4$ , changing  $\epsilon$  by 2 orders of magnitude yields a change of only a factor of 3 in the limit

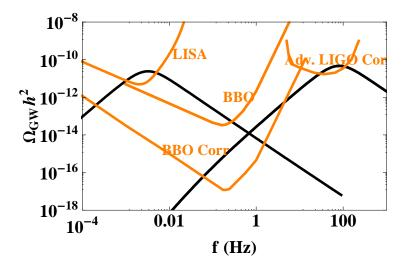


Figure 5. To the GW background from the electroweak phase transition also shown in Fig. 4 (here left black line) we add the result for a phase transition at  $T = 5 \times 10^6$  GeV with  $\Delta \eta_* \mathcal{H}_* = 0.02$  (black curve to the right). In this case, the gravitational wave background might even lie within the reach of advanced LIGO. The sensitivity curves are from [27].

for B.

This limit is unavoidable if the magnetic field on large scales changes simply by flux conservation so that  $B(\eta) = B(\eta_*)(a_*/a)^2$ . Scaling this to today yields  $B(\eta_0) = B(\eta_*)/(1+z_*)^2$ .

The limit is so severe because the magnetic field spectrum is so red. The simple requirement that  $\rho_B(t_*) < \rho_{\rm rad}(t_*)$  yields roughly the same limit. However, this limit is not entirely save since at very early time most of the energy density might in principle have been in the form of small scale magnetic fields which later are converted into heat by viscosity damping on small scales. The fact that such magnetic fields would generate a sizable background of gravitational waves, however, forbids this possibility. This has been realized for the first time in Ref. [28]. The inferred limits on magnetic fields as a function of the spectral index are shown in Fig. 6.

## 5.4. Helicity

The most optimistic dynamo models for the generation of the magnetic fields of about  $10^{-6}$ Gauss which are observed in galaxies and clusters, need seed fields of the order of at least  $10^{-21}$ Gauss. These are excluded by the above limit. There is a possible way out: If the magnetic field has non-vanishing helicity it can develop an inverse cascade and power can be transferred from small to larger scales [29]. In this case the large scale magnetic fields do not simply decay by flux conservation in an expanding universe but they can feed from the small scale fields by inverse cascade.

During the electroweak phase transition parity is broken. Actually, the Chern-Simons winding number of the gauge field,  $N_{CS} \propto \int F \wedge A$ , which is related to the baryon number, has an electromagnetic part to it which is simply the helicity of the magnetic field [30],  $H = V^{-1} \int_V (A \cdot B) d^3x$ . It is interesting to note that this relates the baryon number and the magnetic helicity. It has been shown that the parity violation in the stress energy tensor coming from such helical magnetic fields lead to T-B and E-B correlations in the temperature and polarization spectra of the cosmic microwave background [31]. By the same token they also

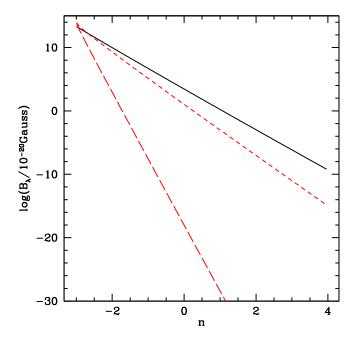


Figure 6. The nucleosynthesis limit on magnetic fields from  $\rho_B(t_{\rm nuc}) < 0.1 \rho_{\rm rad}(t_{\rm nuc})$  (black solid line), and from the gravitational wave constraint (red lines) as a function of the spectral index n. The limits for magnetic fields from the electroweak phase transition are short-dashed (red), while the long dashed (red) line corresponds to magnetic fields from inflation at a GUT scale. Causality requires that the spectral index be n = 2 for magnetic fields from the electroweak phase transition while n is in principle undetermined for inflation. Figure from [28].

generate gravitational waves with non-vanishing helicity [31].

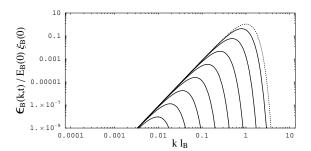
The inverse cascade which is caused by helicity conservation for a helical field and is absent for non-helical magnetic fields has been investigated numerically, e.g., in [32] and is shown in Fig. 7

In Ref. [32] simple power laws are derived for the evolution of the correlation scale in the inverse cascade regime. Using this simple prescription, the mitigation of the magnetic field limits by an inverse cascade of maximally helical magnetic fields has been estimated in Ref. [33]. It has been found, however, that the inverse cascade is not sufficient to present a way out for the magnetic fields from the electroweak phase transition, but it can work for helical magnetic fields generated during the QCD phase transition. The QCD phase transition might be first order if the neutrino chemical potential is large, as discussed in [10].

If the magnetic field is helical, the GW background would not be parity symmetric. There would be more GW's of one helicity than of the other [31].

# 6. Conclusions

- The rapid expansion and collision of bubbles during a first order phase transition stirs the relativistic cosmic plasma sufficiently to lead to the generation of a (possibly observable) stochastic gravitational wave background.
- Observing such a background would open a new window to the early Universe and to high energy physics.



satellite.

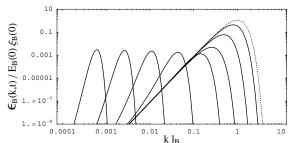


**Figure 7.** Left: the MHD evolution of the large scale magnetic field energy density spectrum with vanishing helicity. The field is simply damped by viscosity on small scales. Large scales are not effected. The viscosity scale is growing with time.

Right: the case of non-vanishing helicity. First, the helicity is relatively small and the evolution of the helical field is not very different from the non-helical case. But due to helicity conservation, helicity rapidly becomes maximal and the evolution enters the inverse cascade regime. For simplicity, the correlation scale is set equal to the damping scale. Figure from [32].

• Generically, the density parameter of the GW background is of the order of

$$\Omega_{gw}(t_0) \simeq \epsilon \; \Omega_{\rm rad}(t_0) \left( \frac{\Omega_X(t_*)}{\Omega_{\rm rad}(t_*)} \right)^2 \; ,$$

where  $\epsilon < 1$  is determined by the duration of the source,  $\epsilon \simeq 1$  if the decay time of the source is roughly a Hubble time.

- The spectrum grows like  $\frac{d\Omega_{gw}(k,t_0)}{d\ln(k)} \propto k^3$  on large scales and decays on scales smaller than the correlations scale  $k_* \sim 1/\Delta \eta_*$ . The decay law depends on the physics of the source.
- Within the standard model, the electroweak phase transition is not of first order and does (probably) not generate an appreciable gravitational wave background. However, simple deviations from the standard model can make it first order.
   In this case we expect a GW background which can marginally be detected by the LISA
- It has been proposed that the magnetic fields generated during the electroweak phase transition, could represent the seeds for the fields observed in galaxies and clusters. Unfortunately this idea does not withstand detailed scrutiny. The magnetic fields cannot have enough power on large scale to represent such seed fields. On small scales the magnetic field power which is initially present is dissipated later on by the viscosity of the cosmic plasma.
- If there is no inverse cascade acting on the magnetic field spectrum, the limits on the large scale fields coming from the generated GW background are too strong to allow significant magnetic fields even for the most optimistic dynamo mechanism.
- If the magnetic field is helical, helicity conservation provokes an inverse cascade which can alleviate these limits. Most probably the relaxed limits are still too stringent for magnetic fields from the electroweak phase transition, but magnetic fields from the QCD phase transition might be sufficient to seed the fields in galaxies and clusters if they are helical.
- Helical magnetic fields generate a parity violating gravitational wave background,  $|h_{+}(k)|^2 \neq |h_{-}(k)|^2$ . This parity violation is in principle observable.

# Acknowledgments

I am grateful to my collaborators Chiara Caprini, Elisa Fenu, Tina Kahniashvili, Thomas Konstandin and Geraldine Servant who worked with me on most of the results reported here. I tremendously enjoyed the many hours of animated and stimulating discussions which helped us to gain insight in this subject which touches on so many fascinating areas of physics. I thank Leonardo Campanelli, Chiara Caprini and Geraldine Servant for helpful comments on a first draft of this paper. Finally, it is a pleasure to thank the organizers of the First Mediterranean Conference on Classical and Quantum Gravity (MCCQG) for inviting me to give this talk and to participate in a lively conference on beautiful Crete. My work is supported by the Swiss National Science Foundation.

# References

- [1] C. J. Hogan, Phys. Rev. Lett. 51, 1488 (1983);
   E. Witten, Phys. Rev. D 30, 272 (1984).
- [2] V. Mukhanov, Physical Foundations of Cosmology, Cambridge University Press (2005).
- [3] Ruth Durrer, The Cosmic Microwave Background, Cambridge University Press (2008).
- [4] Planck URL: http://www.esa.int/Planck
- [5] R. Easther, J. T. Giblin and E. A. Lim, Phys. Rev. Lett. 99, 221301 (2007) [arXiv:astro-ph/0612294];
  - J. Garcia-Bellido, D. G. Figueroa, Phys. Rev. Lett. 98, 061302 (2007) [arXiv:astro-ph/0701014];
  - J. Garcia-Bellido, D. G. Figueroa and A. Sastre, Phys. Rev. D 77, 043517 (2008) [arXiv:0707.0839 [hep-ph]];
  - J. F. Dufaux, A. Bergman, G. N. Felder, L. Kofman, J. P. Uzan, Phys. Rev. D 76, 123517 (2007) [arXiv:0707.0875 [astro-ph]];
  - A. Diaz-Gil, J. Garcia-Bellido, M. Garcia Perez and A. Gonzalez-Arroyo, Phys. Rev. Lett. 100, 241301 (2008) [arXiv:0712.4263].
- [6] K. Rummukainen et al., Nucl. Phys. B532, 283 (1998) [arXiv:hep-lat/9805013];
   K. Kajantie et al. arXiv:hep-ph/9809435.
- [7] C. Grojean, G. Servant, J. Wells, Phys. Rev. **D71**, 036001 (2005) [arXiv:hep-th/0407019];
  - C. Delaunay, C. Grojean, J.D. Wells, JHEP0804:029 (2008) [arXiv:0711.2511];
  - S. J. Huber and T. Konstandin, JCAP0805:017 (2008) [arXiv:0709.2091];
  - J. R. Espinosa, T. Konstandin, J. M. No, M. Quiros, Phys. Rev. **D78**, 123528 (2008) [arXiv:0809.3215];
  - A. Ashoorioon and T. Konstandin, JHEP 0907:086 (2009) [arXiv:0904.0353];
  - T. Stevens and M. B. Johnson, arXiv:0903.2227 [astro-ph.CO], arXiv:1001.3694 [astro-ph.CO];
  - M. Jarvinen, C. Kouvaris and F. Sannino, arXiv:0911.4096 [hep-ph].
- [8] LISA: URL http://lisa.jpl.nasa.gov/
- [9] Y. Aoki et al., Phys. Lett. B643, 46 (2006) [arXiv:hep-lat/0609068];JHEP 0906, 088 (2009) [arXiv:0903.4155].
- [10] D. J. Schwarz, M. Stuke, JCAP 11 (2009) 025 [arXiv:0906.3434].
- A.Boyarsky, O. Ruchayskiy, M. Shaposhnikov, Ann. Rev. Nucl. Part.Sci. 59, 191 (2009) [arXiv:0901.0011].
- [12] G. Hobbs et al., Proceedings of the 8th Amaldi Conference, Class. Quant. Grav. (2010) [arXiv:0911.5206].
- [13] L. Randall and G. Servant, JHEP 0705:054 (2007) [arXiv:hep-ph/0607158].
- [14] LIGO: URL http://www.ligo.caltech.edu
- [15] C. Grojean and G. Servant, Phys. Rev. **D75**, 043507 (2007) [arXiv:hep-ph/0607107].
- [16] A. Kosowsky, M. S. Turner and R. Watkins, Phys. Rev. D 45, 4514 (1992);
  - A. Kosowsky and M. S. Turner, Phys. Rev. D 47, 4372 (1993) [arXiv:astro-ph/9211004];
  - M. Kamionkowski, A. Kosowsky and M. S. Turner, Phys. Rev. D 49, 2837 (1994) [arXiv:astro-ph/9310044].
- [17] C. Caprini, R. Durrer and G. Servant, JCAP 12, 024 (2009) [arXiv:0909.0622].
- [18] C. Caprini, R. Durrer, T. Konstandin and G. Servant, Phys. Rev. D 79, 083519 (2009) [arXiv:0901.1661 [astro-ph]].
- [19] R.H. Kraichnan, Phys. Fluids 7, 1163 (1964).
- [20] D. Biskamp, Magnetohydrodynamical Turbulence, Cambridge University Press (Cambridge, 2003).
- [21] C. Caprini, R. Durrer and G. Servant, Phys. Rev. D 77, 124015 (2008) [arXiv:0711.2593 [astro-ph]].
- [22] S. J. Huber and T. Konstandin, JCAP **0809**, 022 (2008) [arXiv:0806.1828 [hep-ph]].
- [23] R. Durrer and C. Caprini, JCAP **0311**, 010 (2003) [arXiv:astro-ph/0305059].
- [25] R. Durier and C. Caprini, 3CA1 **0311**, 010 (2003) [arXiv.astro-pii/03
- [24] P. Iroshnikov, AZh. 40, 742 (1963);
  - R.H. Kraichnan, Phys. Fluids 8, 1385 (1965).
- [25] C. Caprini and R. Durrer, Phys. Rev. D 74, 063521 (2006) [arXiv:astro-ph/0603476].

- [26] J. Crowder and N.J. Cronish, Phys. Rev. **D72**, 083005 (2005) [ariv:gr-qc/0506015].
- [27] A. Buonanno, arXiv:gr-qc/0303085.
- [28] C. Caprini and R. Durrer, Phys. Rev. D 65, 023517 (2001) [arXiv:astro-ph/0106244];
- [29] A. Brandenburg and K. Subramanian, Phys. Rep. 417, 1 (2005) [arXiv:astro-ph/0405052].
- [30] T. Vachaspati, Phys. Rev. Lett. 87 251302 (2001).
- [31] C. Caprini, R. Durrer and T. Kahniashvili, Phys. Rev. D 69 (2004) 063006 [arXiv:astro-ph/0304556].
- [32] L. Campanelli, Phys. Rev. Lett. 98, 251302 (2007) [arXiv:0705.2308 [astro-ph]].
- [33] C. Caprini, R. Durrer and E. Fenu, JCAP 11, 001 (2009) [arXiv:0906.4976 [astro-ph.CO]].

